INSTITUTO
DE FÍSICA

preprint

PRELIMINARY RESULTS OF THE TBR - SMALL TOKAMAK

I.C.Nascimento, A.N.Fagundes, R.P.da Silva, R.M.O.
Galvão, E. del Bosco, J.H.Vuolo, E. K. Sanada and
R. Dellaqua

Instituto de Física - Universidade de S.Paulo

MAY/80

PRELIMINARY RESULTS OF THE TBR - SMALL TOKAMAK

I.C.Nascimento, A.N.Fagundes, R.P. da Silva, R.M.O.Galvão,

E. del Bosco, J.H.Vuolo, E.K.Sanada and R.Dellaqua

Instituto de Física
Universidade de São Paulo
Caixa Postal 20.516
São Paulo, São Paulo
Brasil

PRELIMINARY RESULTS OF THE TBR - SMALL TOKAMAK

I.C.Nascimento, A.N.Fagundes, R.P. da Silva, R.M.O.Galvão, E. del
Bosco, J.H.Vuolo, E.K.Sanada and R.Dellaqua.

Instituto de Física - Universidade de São Paulo, Laboratório de
Física de Plasmas - Caixa Postal 20516 - São Paulo, São Paulo
CEP-05508 - Brasil

ABSTRACT

The paper gives a short description of the TBR - small
brazilian tokamak and the first results obtained for plasma for-
mation and equilibrium. Measured breakdown curves for hydrogen
are shown to be confined within analytically calculated limits
and to depend strongly on stray vertical magnetic fields. Time
profiles of plasma current in equilibrium are shown and compared
with the predictions of a simple analytical model for tokamak
discharges. Reasonable agreement is obtained taking Z_{eff} as a
free parameter.

1 - INTRODUCTION

TBR is a small research Tokamak designed and construct-
ed at the Institute of Physics of the University of São Paulo
using mainly available granduate student and technician labor
force. The construction began in early 1978 and operation
started in April 1980.

The main objective of the project has been to construct
with resources available in the country a versatile and low cost
device which can be used for research and for trainning of gra-
duate students.

The project and the design of TBR are described in two
reports [1,2]. Design parameters of TBR are given in Table I.

In this paper we present a short description of the
machine and some preliminary results obtained for the plasma
formation and equilibrium.

2 - DESCRIPTION OF TBR

Vessel and Vacuum System

The vessel is constructed using 4 stainless steel 304 L
elbows. Each two of these are welded to form the two halves of
the vacuum chamber. The wall thickness is 3.2 mm and the time

constant for penetration of magnetic field is 320 µs. Four dif-
ferent port configurations are used: retangular 10 x 4 cm² and 6
x 4 cm², 3,8 cm circular and 3,8 cm circular tangential. The
total machine access is 410 cm² for 18 ports. Viton O-rings are
used for seals and also to provide voltage breaks between the
two halves.

The base pressure atained in the vessel is 5 x 10⁻⁷
Torr. The diffusion pump is now being replaced by a 450 l.s⁻¹
turbomolecular pump.

Toroidal field

The toroidal coil is divided into eight sectors, each
containing 14 turns. The two turns at each end of a sector
are half of the thicknesses of the remaining 10 in order to re-
duce field ripple in the gaps between sectors. The coils are
made by silver soldering 5 copper bars to form a "U" (see fig.
1) and a copper bar to close the loop. Each coil is insulated
by winding fiberglass tape and making epoxy impregnation in
vacuum. The electrical connection between adjacent coils is
provided by screwed bars wedges; glued phenolite wedges are
used for insulation. An electrolytic capacitor bank of 4.4 mF x
2790 V (17 kJ) is used to energize the coils. At maximum, the
current is crowbarred with an L/R decay time of 30 ms. Compen-
sation coils are used to reduce stray vertical and radial fields
caused by the toroidal current path and misalignement of coils
(fig. 1, C_3 and C_4 coils).

Ohmic heating

The ohmic heating air core transformer is composed of
three parts: a central solenoid with 48 turns and two flared
sections, at the bottom and top, with 20 turns each. This
design has been chosen to improve the coupling with the plasma
and to reduce stray fields. The transformer is energized with
two capacitor banks: a fast 5 to 60 µF, 10 kV bank and a slow
one of 16,7 mF capacity and 930 V maximum. Passive diode swit-
ching and crowbar are used. Compensation coils are used to
decrease stray fields from the OHT in the plasma region (Fig. 1,
C_1 and C_2 coils).

Vertical field

The coils used to produce the vertical field are shown
in Fig. 1. They are decoupled from OH coils using a solenoid
connected in series and placed in the center of the OHT transfor-
mer. The position of the coils is determined such that a decay
index n of 0,5 is obtained at the center of the plasma. Two
capacitor banks are used to energize the coils: 5 to 65 µF x 3
kV for fast bank and 40 mF x 110 v for the slow bank. Passive
switching and crowbar are used.

Discharge cleaning and preionization

An oscillator of 15 kW and 5 kHz is used to opperate the machine in the discharge cleaning mode. A toroidal DC magnetic field of 200 gauss is maintained during discharge cleaning. The duration and repetition rate of the RF pulses can be varied but usually they are 20 ms and 2 pps. Peak to peak current is 1 kA, filling gas is hydrogen at pressure of a few times 10^{-4} Torr.

In the Tokamak mode, the oscillator is used to produce an oscillating current of 1 kA p-p.

Diagnostics

The diagnostics currently in use are Rogowski, loop voltage, and cosine coils; electrostatic and magnetic probles are sometimes also used. The signals are recorded in storage oscilloscopes. A residual gas analyzer is being installed to monitor the impurities. A Camac System coupled to a PDP 11/45 computer together with a Tektronix video display hard copier system is being installed for data taking. A 65 GHz microwave interferometer, an optical spectrometer, and a soft x-ray detector will be installed whithin one year.

3 - BREAKDOWN CONDITIONS

Breakdown conditions have been studied in TBR in order to identify the best regimes for the operation of the machine and the influence of stray vertical and radial magnetic fields.

In order to obtain the breakdown curves, the OHT fast capacitor bank is fired and the pressure, loop voltage and plasma current are measured. The toroidal magnetic field is fixed at $B_T=1.8$ kG and the voltage of the fast bank is decreased untill no measurable current is obtained. Fig. 2 shows the breakdown curve for H_2. A filament is used as preionizer. Fig. 3 shows the breakdown curve using the oscillator instead of the fast bank, 4,8 kG for B_T, and 6 cm limiter.

The experimental results have been compared with the crude model used by Papoular for discharges in TFR [3]. The electron density in function of time is given by

$$n_e(t) = n_{eo} \exp(\nu-\beta)t$$

where ν is the ionization rate, β the loss rate and n_{eo} the initial electron density. At breakdown, the electron-ion collision frequency is equal to the electron-atom collision frequency. In this case, the critical free electron density is $n_{ecr} \approx 0,1 \, n$, where n is the initial density of neutral atoms.

From the above expression we obtain:

$$t_{cr} = \frac{A}{v-\beta} \quad (2), \qquad \text{where} \quad A = \ln \frac{n}{10n_{eo}} \quad (3)$$

The loss rate β is due to several causes: diffusion recombination, grad B drift and geometrical losses. In general the diffusion and recombination are much smaller than the geometrical β_v, β_r and grad B drift losses β_d. For breakdown:

$$t_{cr} < \frac{1}{\beta_d}, \qquad t_{cr} < \frac{1}{\beta_v}, \quad \text{and also} \quad t_{cr} < t_E, \text{ where } t_E \text{ is the}$$

electric field driving time, and β_d and β_v are grad B drift and geometrical losses respectively.

For t_E it is assumed $t_E = \tau_E/8$, τ_E being the period of the LC circuit of the OHT. Taking $\alpha/p \approx 4$, where α is the first Towsend's coefficient, the following conditions are obtained for TBR:

$$E > 4.1 \times 10^{-2} \text{ V/cm}; \quad E < 8.8 \times 10^6 p^2 - 1.8 \times 10^3 p \quad \text{V/cm} \quad (4)$$
$$p > 1.7 \times 10^{-4} \text{ Torr}; \quad E > 50p \text{ Torr} \quad \text{for} \quad p > 10^{-3} \text{ Torr}$$

These conditions are represented by straight lines in Fig. 2. As we can see, considering the crudeness of the model used, the agreement is reasonable. Interesting characteristics of the curve are the minimum and double value for the breakdown electrical field. For pressures above the minimum of the curve, the mean free path decreases and the electric field is higher in order to provide the necessary ionization rate. For lower pressures the collision rate decrease and the velocity has to increase to keep the ionization rate. The double value of the breakdown electric field is a characteristic toroidal efect caused by the grad B drift. The main disagreement with the model is the limit determined by the grad B losses. But this relation is affected critically by the value of A which in our case has a large error. Another drawback of the model is the use of extrapolated values for the electron drift velocity v from low E/p to high values of E/p. On the experimental side, the determination of stray B_V field and also the value of A are subject to large uncertainties estimated at 10 and 50%, respectively.

4 - INFLUENCE OF STRAY MAGNETIC VERTICAL FIELD ON BREAKDOWN -

During the initial stage of the breakdown, the value of the plasma current is low and the rotational transform is insuficient to short-circuit the electric field caused by the charge separation due to the grad B drift. The existence of a

small vertical magnetic field in order to compensate the $\vec{E} \times \vec{B}$ drift during the initial phase of breakdown can facilitate plasma formation. This equivalent field can be expressed by

$$B_{eq} = \frac{v_d}{v} \, B_T \qquad (6)$$

where v_d is the E drift velocity and v the parallel electron velocity.

This efect has been investigated in TBR by feeding the vertical field coils with DC currents and measuring breakdown voltages for fixed pressure. The stray vertical and horizontal magnetic fields are also measured.

Fig. 4 shows one of these curves for a pressure of 6×10^{-4} Torr. The minimum electric field for breakdown occurs for an external vertical magnetic field of 4 gauss directed down. Fig. 5 shows two breakdown curves: one taken with no external vertical field and the other taken using the optimum vertical field of 4 gauss down, determined from Fig. 4. As we can see, the external field favours strongly the breakdown. With no external field, no breakdown is obtained bellow 5.4×10^{-4} Torr. Considering that the stray vertical field is 6 G up, a net field of the order of 2 G up is necessary to improve breakdown. This is in roughly agreement with B_{eff} calculated from relation (6). Our results are in agreement with the work of Sometani et al [4].

We observe also that a small radial field favours the initial formation of the plasma. For very small radial field, approximately 3 G for $B_T = 1.8$ kG, we can not have breakdown. Using only one radial field compensating coil on top and bottom in series with the toroidal coil, instead of two we have increased the radial field to 13 G, directed to the inside, and good breakdown curves have been obtained. Possibly, the displacement of the toroidal field lines to the inside of torus caused by the radial component of B_T, introduces an electron drift that facilitates the breakdown.

5 - PLASMA EQUILIBRIUM

The experiments in the Tokamak regime comprehended two phases: the first between May and October 80 using a limiter of half a ring shape of 6 cm radius and the second, between November 80 and January 81 with a ring limiter of 8 cm radius. In February the machine was dismounted in order to replace the diffusion pump by a turbomolecular pump and to install helical coils around the vessel.

Fig. 6 shows three typical shots for plasma current, and loop voltage. Plasma position is shown for shots a and b. Experimental conditions are shown in Table 2. The experiments have been performed with hydrogen gas flowing continuously.

Plasma equilibrium is searched by changing the values of the parameters of the fast and slow OH and vertical field capacitor banks. Adjustements by trial and error are made varying the voltages and triggering time of these banks in an iterative way. Plasma densities are calculated from the filling density and the temperature from Spitzer's formula at $I_{p\ max}$. Both are average values.

Fig. 6a indicate that the plasma is centered and in equilibrium for about 2 ms; however, part of the current has been probably cut out by the limiter in the beginning of the pulse. Fig. 6b shows a long pulse but with the plasma column changing position. Fig. 6c shows MHD activity while in Figs. 6a and 6b MHD activity is lower. In the majority of the shots, the lack of good equilibrium is probably due to the slow penetration time of the vertical field as compared with the rise time of the current. A NaI scintillator detector installed near the limiter has shown a high intensity of hard x-rays indicating runaway dominated discharges.

Plasma currents shown in Figs. 6a and 6b are compared with the predictions of an analytical-numerical model [5].

The tokamak ohmic heating system can be modelled as two coupled electrical circuits. The differential equations describing the behaviour of these circuits are non-linear because the plasma resistance, R_p, depends on the plasma current through the electron temperature, T_e. In the model, the circuit equations for R_p fixed are solved analytically and a numerical difference scheme is used to calculate the time dependence of R_p. At each time step, R_p is calculated from T_e using the expression for the plasma resistivity derived by Hirschman [6], which is valid for all tokamak transport regimes. This value of R_p is then used in the analytic solution of the circuit equations to advance the plasma current in time. Once the plasma current, and hence the ohmic power input to the plasma, is known, a new value of T_e may be calculated from the finite difference approximation to the plasma transport equations. The radial profiles of the plasma quantities are chosen a priori as parabolic and assumed constant during the plasma lifetime.

Figs. 7 and 8 show the calculated time evolution of the plasma current for several effective Z and experimental values shown in Figs. 6a and 6b. As we can see, there is better agreement for $Z_{eff} \sim 4$. From the model, the average temperature obtained is $T_e \sim 150$ eV, while using Spitzer's formula with $Z_{eff} = 4$ the value for T_e is 75 eV. Confinement time is roughly 0.5 ms for Z=4, in agreement with the predicted value of 0.7 ms from the empirical sealing laws given by Hugill and Sheffield [7].

6 - CONCLUSION

The first results from the operation of TBR indicate that the parameters of the design were attained. There are difficulties with the vertical field for equilibrium which is very critical. Also, the reproducibility of the shots is not good and most of the discharges are runaway dominated. Presently, the machine is being reassembled. The vessel was electropolished and a turbomolecular pump is going to be used. With glow discharge and discharge cleaning it is expected to decrease Z_{eff} and improve the reproducibility of shots. The vertical field system is going to be modified to include feedback stabilization.

ACKNOWLEDGMENTS

REFERENCES

1) Nascimento, I.C.; Galvão, R.M.O.; Fagundes, A.N.; Vuolo, J.H. and Prates, R.M.P. - Instituto de Física da USP, Laboratório de Física de Plasmas, Report LFP-1 (1977).
2) Simpson, S.W.; Nascimento, I.C.; Galvão, R.M.O.; Silva, R.P.da; Drozak, R.M.P.; Fagundes, A.N. and Vuolo, J.H. - Instituto de Física da USP, Laboratório de Física de Plasmas, Report LFP-2 IFUSP/P-155 (1978).
3) Papoular, R. - Nucl.Fusion 16, (1976) 37.
4) Sometani, T. and Fujisawa, N. - Plasma Phys. 20, (1978) 1101.
5) Drozak, R.M.P.; Galvão, R.M.O. and Nascimento, I.C. - Rev.Bras. Física 10, (1980) 851.
6) Hirschman, S.P.; Hawriluk, R.J. and Birge, B. - Nucl.Fusion 17, (1977) 611.
7) Hugill, J. and Sheffield, J. - Nucl.Fusion 18, (1978) 15.

TABLE I

MAIN PARAMETERS OF TBR

Major Radius	R	0.30 m
Vessel Radius	a_v	0.11 m
Plasma Radius	a	~0.08 m
Aspect Ratio	R/a	4
Toroidal Field	B_ϕ	5 kG (±6% in τ_I)
Poloidal Field	B_θ	500 G
Vertical Field	B_z	230 G
Plasma Current	I_p	20 kA
Current Duration	τ_I	4 ms
Electron Density	n_e	~2 x 10^{13} cm^{-3}
Electron Temperature	T_e	~240 eV
Ion Temperature	T_i	~70 eV
Confinement Time |7|	τ_E	~0.7 ms

TABLE II

SUMMARY OF RESULTS

	FIG.6a	FIG.6b	FIG.6c
B_T (kG)	5.3	5.3	5.3
Filling pressure (Torr)	1.0×10^{-4}	2.1×10^{-4}	2.3×10^{-4}
Density (cm^{-3})	6.5×10^{12}	1.4×10^{13}	1.5×10^{13}
$I_{p\ max}$ (kA)	4.0	7.7	7.2
V_{loop} (V) (at $I_{p\ max}$)	5.5	4.7	2.5
T_e (eV) (Z=1)	17	20	30
Pulse lenght (ms)	3.8	7.4	7.3
Limiter radius (cm)	6	8	8
q (a)	8.0	7.3	7.8
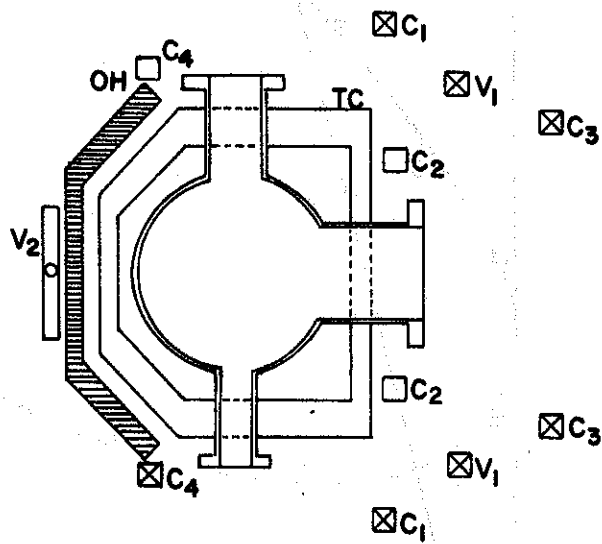
Fig. 1 - Cross section of TBR. Coils C_1, C_2, C_3 and C_4 are stray field compensating coils; V_1 and V_2 are the vertical field coils, and OH is the central ohmic heating bobbin.
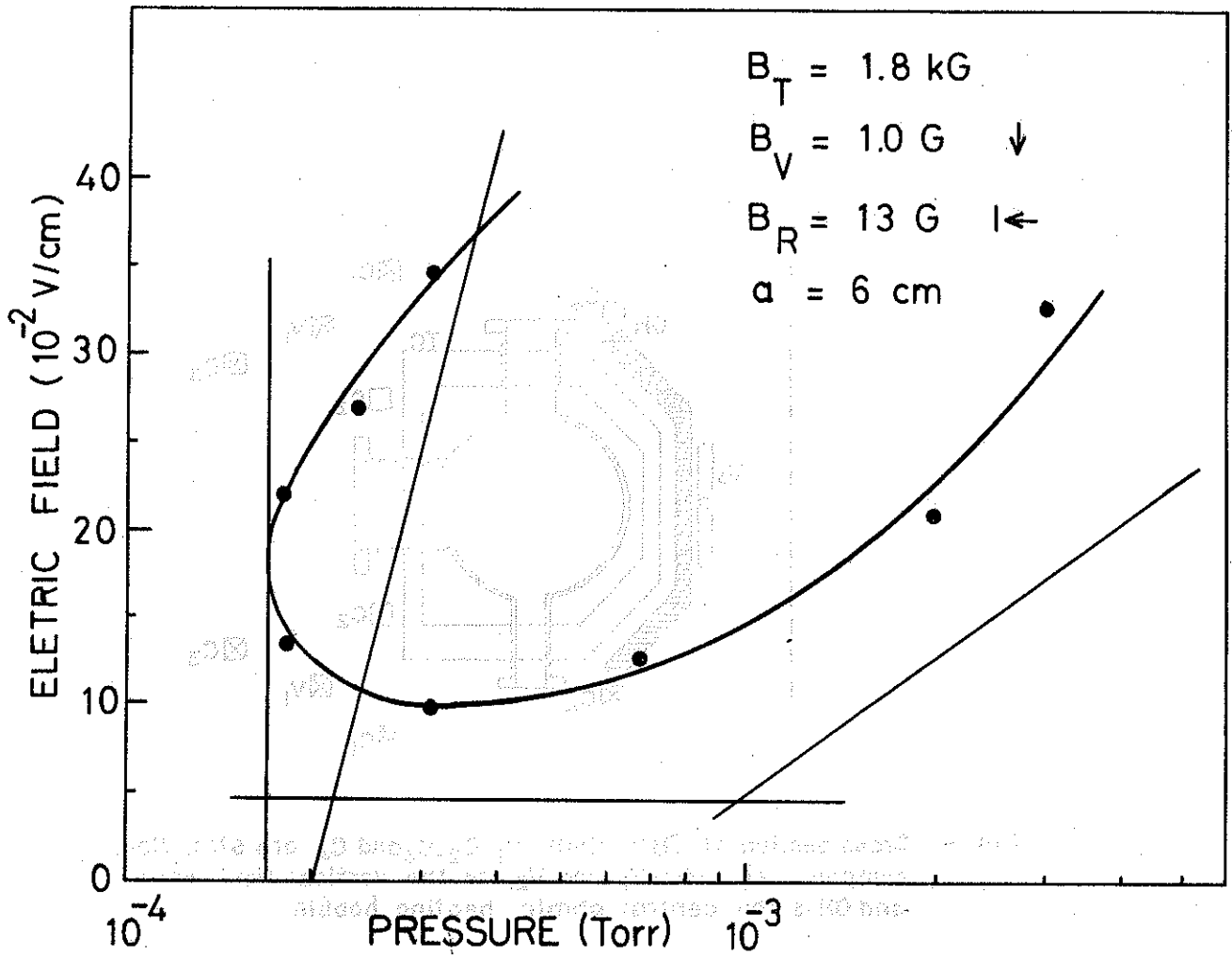
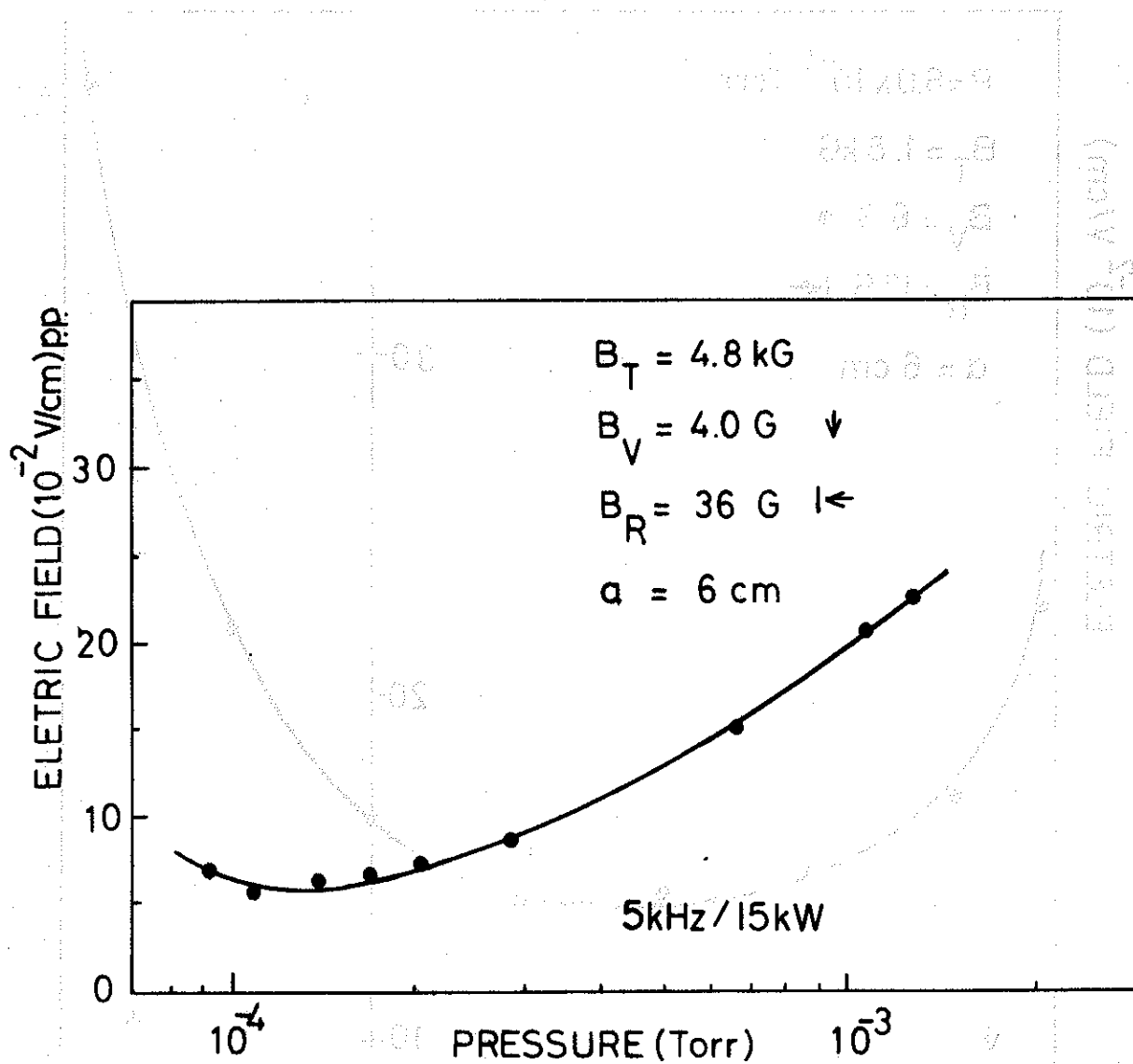Fig. 2 - Breakdown curve for H_2 with the fast bank.
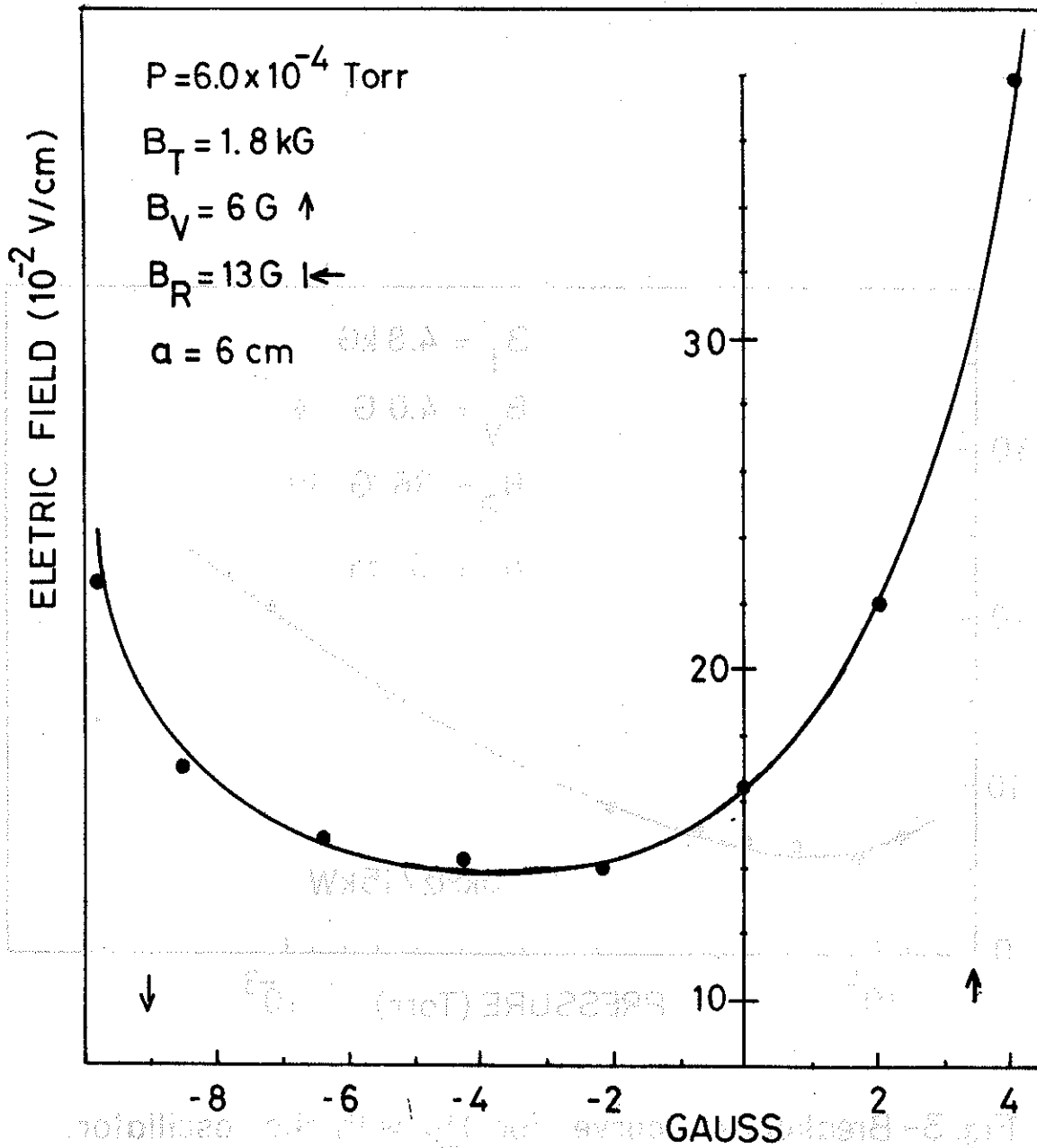
Fig. 3- Breakdown curve for H_2 with the oscillator.

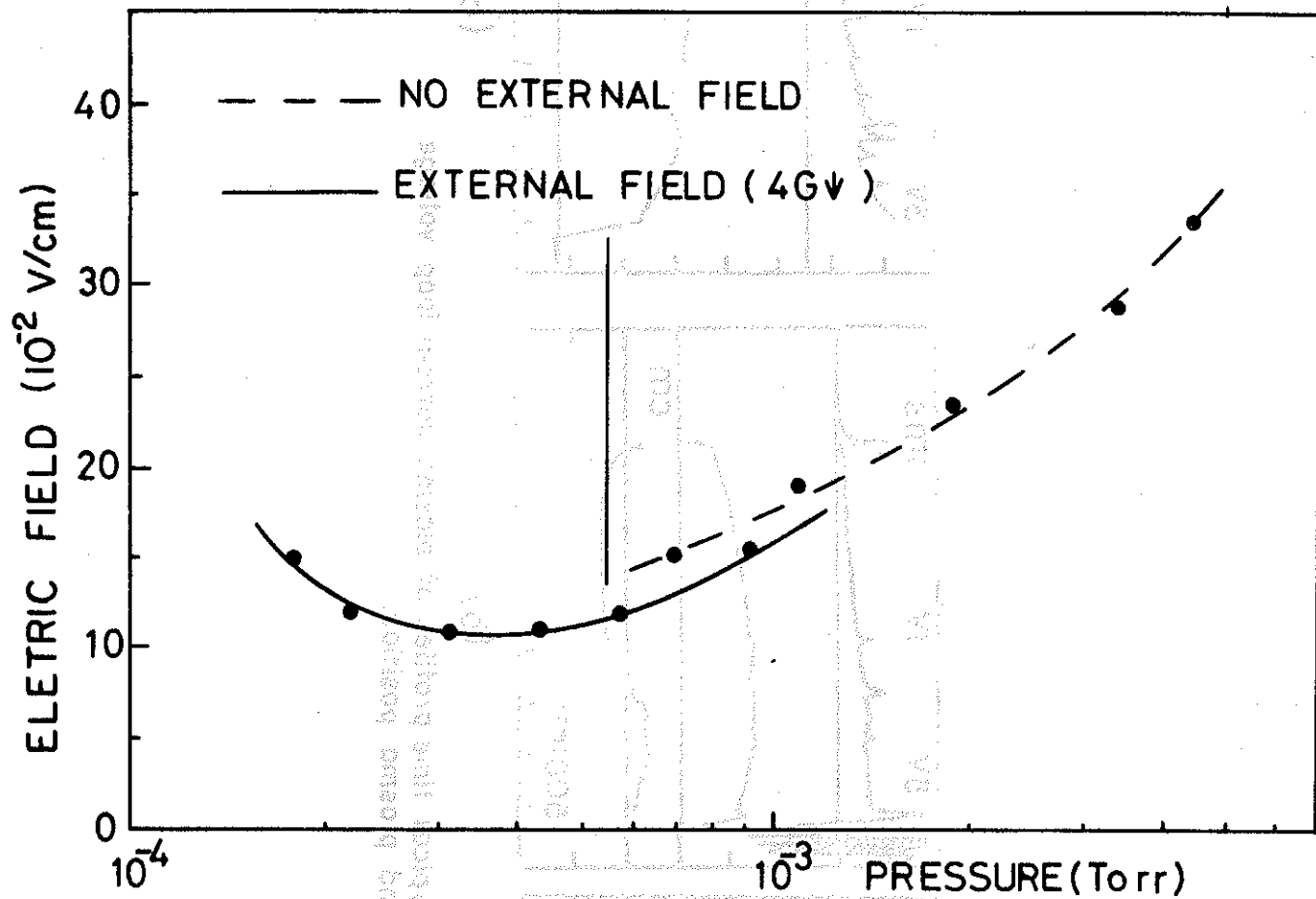Fig. 4 - The influence of an external vertical field on hydrogen breakdown.

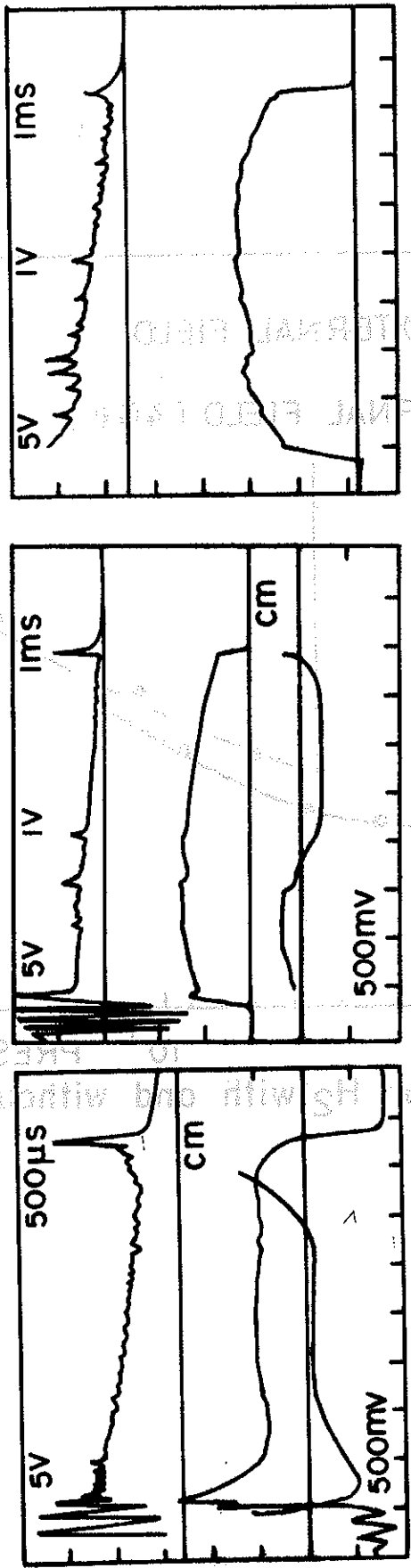Fig. 5 - Breakdown curves for H_2 with and without optimized vertical field.

Fig. 6 – Typical time profiles of plasma current, loop voltage and plasma position.

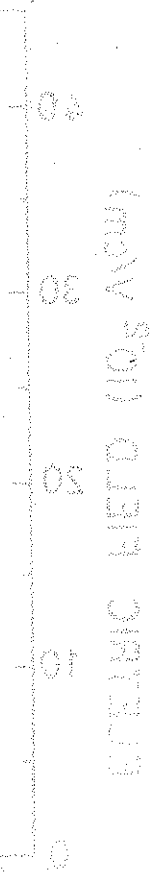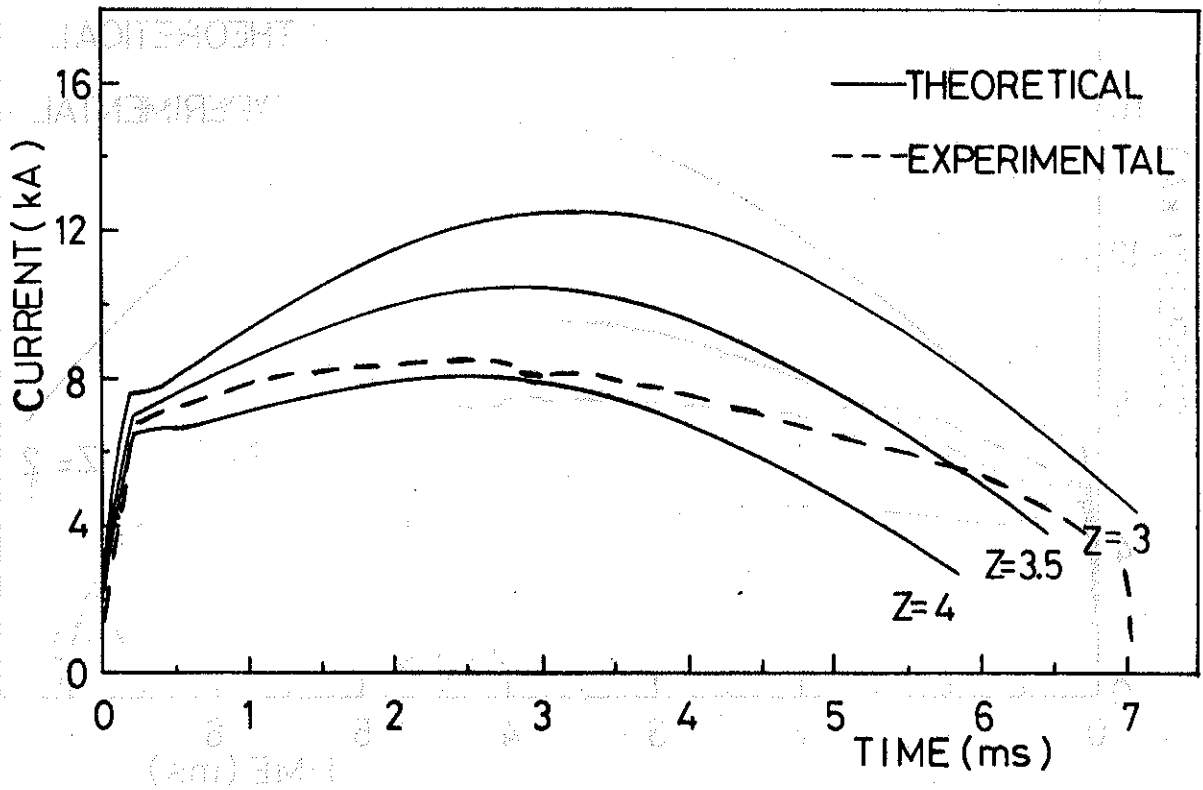Fig. 7 - Comparision between the analytical-numerical model predicted plasma current and measured values of Fig. 6b.
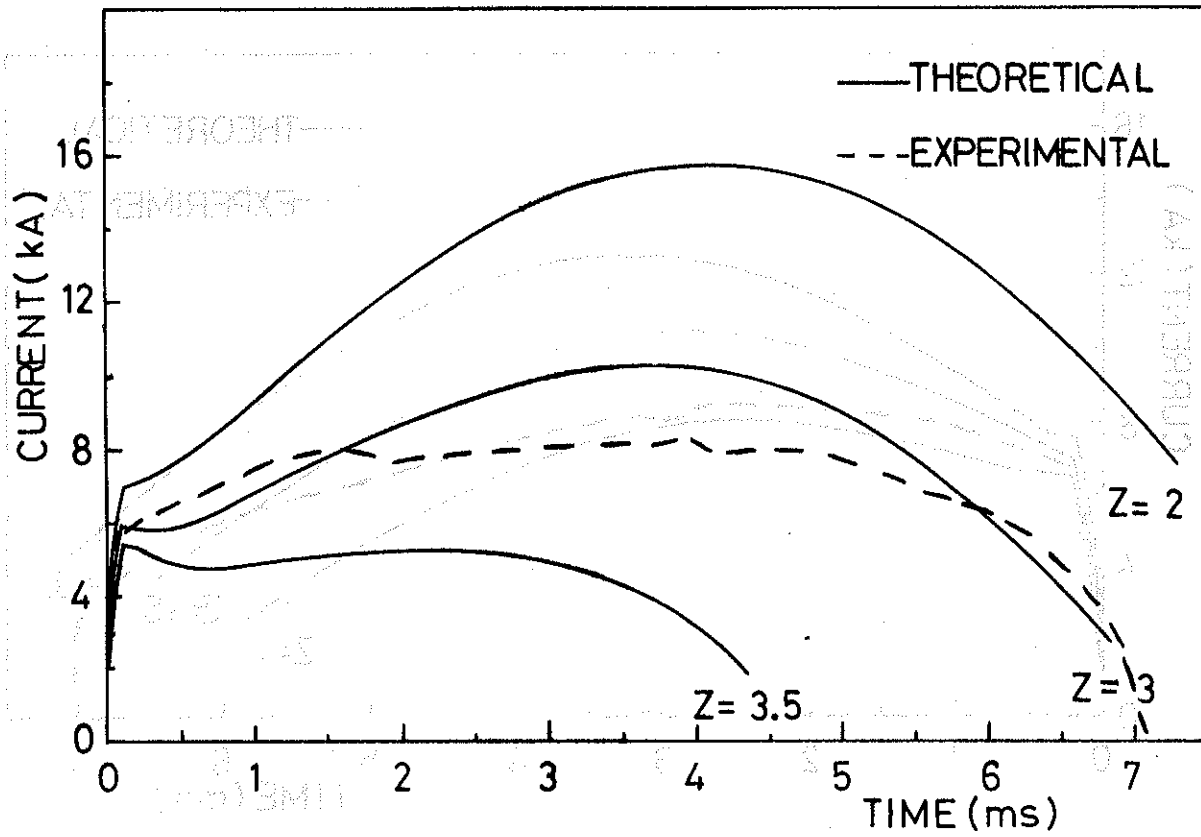
Fig. 8 - Comparision between the analytical-numerical model predicted plasma current and measured values of Fig. 6c.